REPORT

A computational method for quantifying morphological variation in scleractinian corals

K. J. Kruszyński · J. A. Kaandorp · R. van Liere

Abstract Morphological variation in marine sessile organisms is frequently related to environmental factors. Quantifying such variation is relevant in a range of ecological studies. For example, analyzing the growth form of fossil organisms may indicate the state of the physical environment in which the organism lived. A quantitative morphological comparison is important in studies where marine sessile organisms are transplanted from one environment to another. This study presents a method for the quantitative analysis of three-dimensional (3D) images of scleractinian corals obtained with X-ray Computed Tomography scanning techniques. The advantage of Computed Tomography scanning is that a full 3D image of a complex branching object, including internal structures, can be obtained with a very high precision. There are several complications in the analysis of this data set. In the analysis of a complex branching object, landmark-based methods usually do not work and different approaches are required where various artifacts (for example cavities, holes in the skeleton, scanning artifacts, etc.) in the data set have to be removed before the analysis. A method is presented, which is based on the construction of a medial axis and a combination of image-processing techniques for the analysis of a 3D image of a complex branching object where the complications mentioned above can be overcome. The method is tested on a range of 3D images of samples of the branching scleractinian coral *Madracis mirabilis* collected at different depths. It is demonstrated that the morphological variation of these samples can be quantified, and that biologically relevant morphological characteristics, like branch-spacing and surface/volume ratios, can be computed.

K. J. Kruszyński · R. van Liere
Center for Mathematics and Computer Science,
Kruislaan 413, 1098 SJ Amsterdam, The Netherlands

J. A. Kaandorp (✉)
Section Computational Science, Faculty of Science,
University of Amsterdam, Kruislaan 403,
1098 SJ Amsterdam, The Netherlands
e-mail: jaapk@science.uva.nl

Introduction

Marine sessile organisms from very different taxonomical groups show considerable morphological variation. This variation is often related to gradients in environmental conditions such as light intensity and water flow velocity. The growth form in the reef-building corals *Montastraea annularis* and *Porites sillimaniani* is influenced by light intensity (Graus and Macintyre 1982; Muko et al. 2000). Similarly, growth forms of octocorals, hydrozoans, sponges and some branching species of coral have been shown to vary along gradients of water flow and/or nutrient availability (de Weerdt 1981; Kaandorp and de Kluijver 1992; Lesser et al. 1994; Sebens et al. 1997; Kaandorp et al. 2003; Kim et al. 2004). Quantifying how morphology changes in response to environmental conditions is relevant in a range of ecological studies. For example the growth form of fossil material (Stearn and Riding 1973) can be

used to estimate the state of the physical paleo-environment. A quantitative morphological comparison is important in studies where marine sessile organisms are transplanted from one environment to a different one (de Weerdt 1981; Graus and Macintyre 1982; Kaandorp and de Kluijver 1992; Muko et al. 2000). Morphological variation can involve various biologically relevant structures, for example in arborescent corals, the diameter of the branches, branching rate, branching angles and branch spacing (Bruno and Edmunds 1998). In studies on the influence of hydrodynamics on the particle capture in the branching scleractinian coral *M. mirabilis* (Sebens et al. 1997), it was demonstrated that branch diameters and branch spacing are crucial morphological properties. The diameter of the branches and spacing between branches is variable, and may be controlled by a combination of hydrodynamics and genetics. Sebens et al. (1997) argue that through modifications of its branch structure and branch spacing, *M. mirabilis* can function efficiently as a passive suspension feeder over a wide range of exposure to water movement. Models of growth and form of branching scleractinian corals and the influence of the physical environment have been developed in a number of studies (Merks et al. 2003; Kaandorp et al. 2005). Robust methods for quantitative comparison of simulated and real morphologies are an important prerequisite for verification of models that simulate coral growth.

Existing techniques for measuring morphology and surface area of organisms with complex colony shapes have several limitations. One approach is to tightly wrap the object with aluminum foil (Marsh 1970) or a thin sheet of latex rubber (Meyers and Schultz 1985) and to determine the surface area using a surface-area-to-mass calibration. An alternative approach is to dip the object in molten wax (Stimson and Kinzie 1991) or dye (Hoegh-Guldberg 1988) and to analyze the amount of adhering material. Both of these methods are destructive, are not necessarily very precise and provide only information on surface area, therefore overlooking a number of important morphological parameters. More recently, computer techniques have been developed for the analysis of organism shape. There are some two-dimensional (2D) methods that can quantify branching patterns (Kaandorp 1999; Abraham 2001; Sanchez and Lasker 2003; Shaish et al. 2006). An important limitation of the 2D studies is that this method only works well for growth forms which tend to form a branching pattern in one plane, for example the sponge *Raspailia inaequalis* analyzed by Abraham (2001). This method does not provide optimal results for many scleractinian corals, where usually three-dimensional (3D) branching structures are formed with branches in all directions, as for example in *M. mirabilis*. Moreover, 3D methods based on 3D reconstruction using underwater photography of coral colonies (Bythell et al. 2001) and bryozoan colonies (Cocito et al. 2003) have
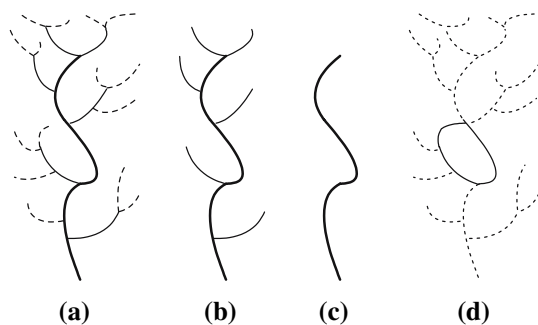
become available. Overlapping images completely encircling the specimen are required for the reconstruction. The number of photographs increases with the complexity of the object. Complex branching organisms cannot be adequately modeled with this technique since due to occlusion effects, some branches of the growth form may overlap other branches, and it is impossible to obtain complete photographic coverage of the entire surface. The advantages are that the method is non-destructive, is applicable in fieldwork, and can be used to measure many morphological parameters. One limitation is the time-consuming nature of the process. The time needed to process an object increases with its complexity and may require 3–4 h (Bythell et al. 2001) or 3 h (Cocito et al. 2003) and the method can only be applied to analyze non-branching forms. For the morphological analysis of complex branching organisms 3D computer imaging methods are required, as for example X-ray computed tomography (CT). With these techniques it is possible to capture information on the internal structure of the organism in the form of slice-planes similar to conventional photographic X-rays and by using sophisticated mathematical techniques the object can be reconstructed in three dimensions. The advantage of CT-scanning is that a full 3D image of the object, including internal structures, can be obtained with a very high precision. A particular advantage of CT scanning is that it is especially suitable to investigate calcified structures and to measure skeletal densities (Vago et al. 1994). The precision depends on the type of CT scanner but can be mm (medical scanner) to microns (micro CT scanner). Although CT scanning is also suitable for living material, in practice in research on marine sessile organisms it is mainly used to analyze dead material in a non-destructive way. A problem with the morphological analysis of CT scans is the complexity of the acquired data set, which requires special image processing and morphometric methods.

An important complication in the morphological analysis of growth forms of scleractinian corals and many other marine sessile organisms is that the growth forms are usually indeterminate and complex. Most methods for the analysis of growth and form use landmark-based geometric morphometrics (Bookstein 1991). These methods are more suitable for unitary organisms and less applicable for the analysis of indeterminate growth forms of modular organisms (Harper et al. 1986). In a number of cases, the organism is built from well-defined modules (for example the corallites and polyps in scleractinian corals). In other cases, the module itself has no well-defined shape but an irregular and indeterminate form (for example an osculum and its corresponding aquiferous system in sponges). For organisms with well-defined modules it is possible to apply landmark-based methods for the morphometrics of individual modules. For example, Budd et al. (1994) and Budd and

Guzman (1994) used landmark-based methods to measure the corallites in a scleractinian coral while Todd et al. (2001) measured the morphological variation of the polyps in a scleractinian coral.

This paper describes a new approach for analyzing 3D images of branching objects based on morphological skeletons (an overview of these methods is provided by Jonker and Vossepoel 1995). The morphological skeleton can be obtained with an image-processing algorithm. Skeletonization algorithms reduce the object to a network of thin lines, one pixel or voxel thick, running through the centers of the object (Fig. 1a). A morphological skeleton or medial axis has the same topology (a similar branching structure) as the original object, and occupies the same spatial extent in the image. The algorithms can work on 2D as well as on 3D images, resulting in 2- and 3-D skeletons, respectively. A skeleton resulting from a skeletonization algorithm is shown in Fig. 1a, where the original branching object is simplified into a line graph. There are several problems and pitfalls in the construction of morphological skeletons. A major unresolved issue is that the skeletonization algorithm may result in a morphological skeleton with a higher degree of topological complexity than present in the original branching organism. This type of skeleton is virtually useless for measurement and visual inspection of the data. The other major issues are the presence of various artifacts (for example cavities and holes in the coral skeleton, scanning artifacts, etc.) and the lack of a mechanism for the interactive or automatic removal of loops in the morphological skeleton (Kaandorp and Kübler 2001).

The aim of this paper is to present a procedure for the quantitative analysis of 3D images of complex-shaped organisms obtained with CT scanning techniques. The quantitative analysis is based on measurements related to the 3D morphological skeleton (see Fig. 2). A brief description is given of the various algorithms which were applied to the 3D image to obtain a morphological skeleton which

(a) approximates the medial axis of the object as closely as possible; (b) can be used to define biologically relevant measurements; (c) can be used for the visual inspection of the data. In the measurement procedure several visual inspection steps are required. These steps will be described, as well as the procedure from 3D image to the final list of measurements, including the potential pitfalls in this process. As a case study an analysis has been made of morphologies of *M. mirabilis* colonies collected at different depths (see Fig. 3). *M. mirabilis* is characterized by a relatively complex-shaped branching morphology and a certain, depth related morphological plasticity (Bruno and Edmunds 1998). The *M. mirabilis* representations in Fig. 3a and c differ greatly in their compactness, and it is assumed that the object shown in Fig. 3b constitutes an intermediate form between these two (Kaandorp and Kübler 2001). This species is a suitable case study to test whether the presented quantification method can be applied in a realistic biological scenario.

Materials and methods

Three-dimensional data acquisition

The *M. mirabilis* colonies were collected at depths between 6 and 20 m at the reef of Curaçao (Netherlands Antilles, 12°N 69°W). The colonies were cleaned and the skeletons were transported to Amsterdam. Three-dimensional images of the colonies were obtained using X-ray CT scanning techniques (Kaandorp and Kübler 2001). A medical scanner (Philips Mx8000) was used. The morphological analysis system has been applied to measure the three specimens of *M. mirabilis* shown in Fig. 3. The three coral colonies were scanned at a (nearly isotropic) resolution of 0.25 mm × 0.25 mm × 0.3 mm with a slice size of 512 × 512 pixels. An isotropic resolution is obtained by using equal slice spacings in all dimensions. Due to technical limitations in medical scanners, anisotropic resolutions are frequently used and a lower resolution is applied in one dimension. In the reconstruction process the higher resolution in the other dimensions is used to approximate the object. By applying a nearly isotropic resolution this approximation could be avoided. The numbers of slices in the samples shown in Fig. 3a–c were 329, 541 and 373 in each scan, respectively.

Artifacts in the three-dimensional images

There are three sources of artifacts in the 3D data set: (1) artifacts caused by damage to the coral skeleton due to fracture of the skeleton, boring activities of other organisms and erosion processes; (2) anastomosis of branches and

Fig. 1 Horton-Strahler branch ordering. **a** Shows a simple network. **b** Is created by removing all outermost branches from the network in (**a**), these same branches being denoted as "first order branch segments". The new "leaves" in the pruned network of (**b**) are labeled as second order branch segments and are themselves removed to give **c** a third order branch segment. **d** A network with a loop

Fig. 2 a Branch thickness, diameter *da* of sphere *a* (*white sphere*) located at each branching point, diameter *db* of sphere *b* (*black sphere*) directly adjacent to sphere *a*, and diameter *dc* of sphere *c* (*gray sphere*) at the end of terminal branches. **b** Branching angle *b_angle*, between the centers of sphere *a* and adjacent spheres *b*. **c** Geotropy angle *g_angle*, between the line connecting successive spheres *a* and the positive *y*-axis (*dashed line*). The *solid lines* also indicate the branching rate *rb*. **d** Branch spacing, radius of a sphere at the tip of a branch
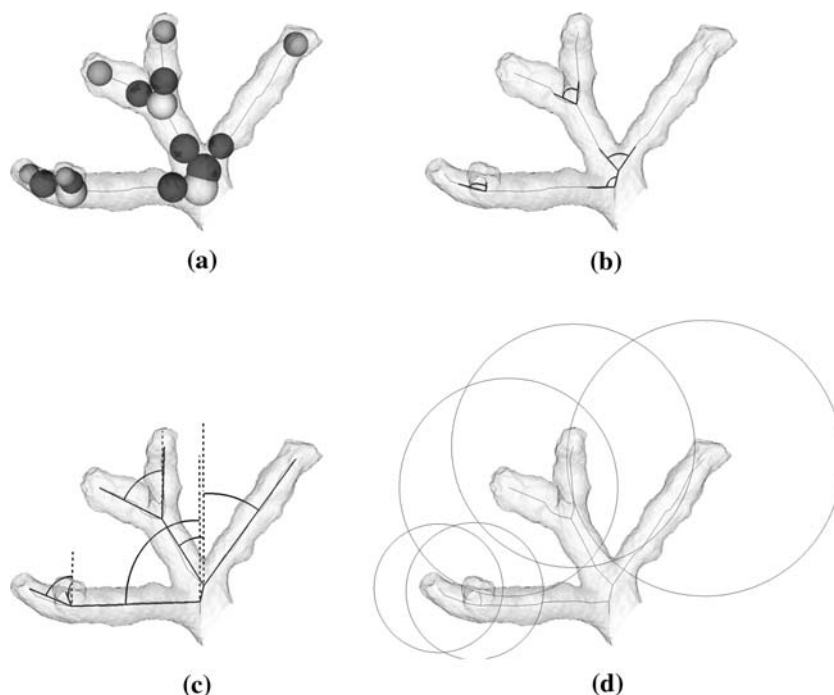
surface rugosity are natural properties of the skeleton but introduce complications into the analysis that must be rectified; (3) artificial fusing of branches due to scattering of X-rays during the scanning process. In the Electronic Supplementary Material a discussion can be found of the various types of artifacts, and the methods which were applied to remove these artifacts from the data set. A more detailed and technical discussion can be found elsewhere (Kruszyński et al. 2006).

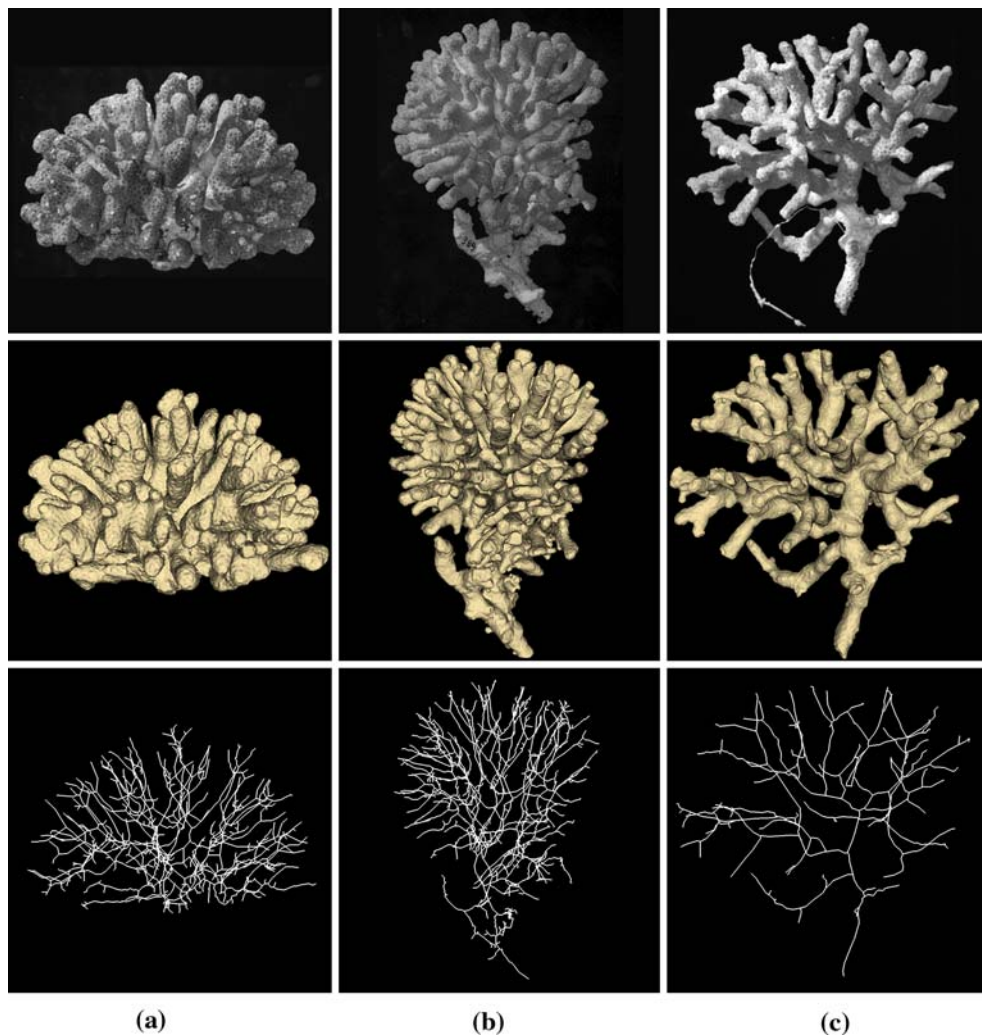Processing of the three-dimensional images

In order to reduce the number of noise-related artifacts in the data set, the images were subjected to four iterations of the Curvature Flow noise reduction algorithm from the Insight Segmentation and Registration Toolkit (ITK, Ibanez and Schroeder 2003). The resulting data was then segmented with the ITK Confidence Connected algorithm. Segmentation entails dividing images into regions which are occupied by an object (the coral colony), and regions which are not occupied by the object. This enables the subsequent extraction of a skeleton from an image. A hole-filling algorithm was then applied to the images to remove the previously mentioned damage-related artifacts. This algorithm is briefly explained in the Electronic Supplementary Material.

Morphological analysis using skeletonization

In the literature several algorithms have been proposed for constructing morphological skeletons in 3D images. In

Kruszyński et al. (2005) a comparison can be found of a number of well-known algorithms and a quantification of how well these algorithms approximate the medial axis of a 3D object. In this comparison the algorithm by Xie et al. (2003) appeared to be the best. The medial axis of the branching object can be used for various measurements. The medial axis structure can be used to analyze the branch ordering (Horton 1945; Abraham 2001). Branch ordering can be defined algorithmically. In this definition one is moving from the outermost parts of the network inwards, counter to the direction of growth. In the first step, the outermost branches are labeled as the first order branches (Fig. 1a), after which they are pruned from the network. In the second step, the new outermost branches are labeled as second order branches (Fig. 1b) and these are removed as well. This process continues increasing the order by one for each step and removing the branches until no branches remain. The network is then reassembled and the order of each branch in the network is now known. The definition can be used to order the branches in a hierarchical way and to define the stem or "root" of the network. In the example of Fig. 1, the root is found in three pruning steps (Fig. 1c). It is not possible to determine the ordering of a network containing loops (Fig. 1d). After a number of steps a network containing only loops remains without any branches.

The hierarchical ordering in Fig. 1 can be used to measure various biologically relevant parameters such as the diameter of the branches, branching rate, branching angles and branch spacing. Figure 2 shows how these measurements are obtained. Figure 2a shows the branch thickness. This is determined by measuring the diameter *da* of spheres

Fig. 3 Result of the processing of the three *Madracis mirabilis* samples, from *left* to *right*: **a** compact-shaped morph collected at 6 m depth; **b** compact morph collected at 15 m; and **c** the thin-branching morph collected at 20 m. The dimensions of the samples are respectively 10 cm × 7 cm × 9 cm, 11 cm × 16 cm × 12 cm, and 11 cm × 11 cm × 10 cm. The *top row* shows photographs of the colonies. In the *middle row* surface renderings of the segmented volumes are shown, and the *bottom row* shows the final skeleton after removal of loops and other artifacts

a located at branching points (white sphere), and the diameter *db* of spheres *b* located directly adjacent to those (black sphere). The measurements *da* and *db* indicate respectively, the maximum and minimum branch thickness. In addition, the diameter *dc* of the sphere *c* located at the endpoints of the morphological skeleton (gray sphere) is determined. The thickness *dc* indicates the thickness of branches added most recently to the colony and can be used to detect recent changes in the growth process. The measurement *rb* is the branching rate, and is defined by the length of an edge connecting the centers of two successive *a* spheres. A low value of *rb* indicates a high branching rate, while high values indicate a relatively slow formation of branches during the growth process. Two types of angles are measured using the skeleton: *b_angle* is the branching angle, and is defined by the center of each sphere *a* and the centers of

adjacent spheres *b* (see Fig. 2b); *g_angle* is the geotropy angle and is defined by the angle between the vector connecting the centers of two successive *a* spheres and the positive *y*-axis (see Fig. 2c). The *y*-axis in the construction of *g_angle*, shown as dashed lines in the figure, corresponds to the original growth position and is directed away from the substrate. The angle *g_angle* expresses the degree of substrate tropism. Low values of *g_angle* reflect a high degree of negative substrate tropism with branches of the organism showing a tendency to develop away from the substrate. The diameter *br_spacing* is defined as the radius of the smallest possible sphere, located at the tip of a first order skeleton branch, such that the section of the morphological skeleton inside the sphere consists of at least two disjoint parts (Fig. 2d). The circles in the figure correspond to the radius of these spheres, centered at the tips of the branches.

The standard deviation of *br_spacing* expresses the degree to which branches tend to fuse. A relatively low value indicates that there is a low degree of self-intersection between branches while a high value shows that there is no mechanism present preventing self-intersection and fusing (anastomosis) of branches may occur. In a number of cases the value of *br_spacing* is undefined, for example when the tip of the root of the object shown in Fig. 1c is used as the center of construction (*br_spacing* will be infinitely large). In morphological measurements these non-valid centers are not used. In all definitions mentioned above it is assumed that the branches are ordered in a hierarchical way, and branches are not fused, thus creating loops in the skeleton. All points of anastomosis have to be removed before the measurements can be done.

Skeletonization, skeleton graph processing and measuring

From the processed 3D images a 3D morphological skeleton was extracted using the skeletonization algorithm proposed by Xie et al. (2003). The morphological skeleton was converted into a graph representation (Reinders et al. 2000). The next step was the removal of loops from the skeleton. The measurements shown in Fig. 2 require the skeleton branches to be ordered. This is only possible if the skeleton contains no loops, but this is usually not the case. To the knowledge of the authors, there is currently no algorithm available to detect the exact location of fusion points of branches in the morphological skeleton. Loops were detected automatically in the branch ordering process, and user interaction was required to indicate the location and the size of the necessary disconnection in the morphological skeleton. Finally, to enable correct measurements, the root of the coral was selected manually and the proper orientation of the coral with respect to the ground was established interactively. After this the skeleton was used to measure the coral colony using the quantities described in Fig. 2.

The Visualization Toolkit (VTK, Schroeder et al. 1997) was used to show the results of the image processing and for the visual interaction with the data set in the entire procedure. The system was implemented in C++ and Python, and runs under a Linux operating system. A first version of the 3D morphological analysis system will be made available on a website (Kaandorp 2007).

Statistical analysis

The distribution of the measurements was investigated by applying nonparametric methods which can be applied to various types of distributions. The distributions were compared by applying a two-sample rank test. The advantage of this test is that its result is not influenced by differences in skewness and kurtosis of the investigated distributions. In all cases the hypothesis that the distribution of measurements of both objects is the same is tested against the alternative that they differ by a translation.

Results

The variation in numerous measures of colony morphology of *M. mirabilis* detected by the analysis procedure was consistent with previously observed trends of morphological variation for this species. The largest branch spacing (*br_spacing*) was found in the thin-branching deep-water morphology, and the branch spacing of the samples increased with depth (Table 1; Fig. 4). Across the same depth range the standard deviation of the branch spacing also decreased, indicating a more regular branching pattern (Table 1; Fig. 4). For the sample from deep water, there were no values close to zero for this parameter, which demonstrates that no anastomosis was present in this colony (something which could be verified in the loop removal procedure discussed in the methods), while for the intermediate and shallow depth samples, values near zero occurred and anastomosis of branches did occur. When the standard deviations of the measurements of the geotropy angles (*g_angle*) and the branching angles (*b_angle*) were compared (Table 1), it was observed that with decreasing depth branches tended to form in almost all directions, while in deep locations most branches would be formed in vertical directions. The branching rate (*rb*) increased with decreasing depth (Table 1; Fig. 4). The more compact shallow and intermediate depth morphs were characterized by a relatively higher degree of branch formation. The measurements on the minimal (*db*), maximal (*da*), and terminal thickness of branches (*dc*) all showed a similar tendency (Table 1; Fig. 4) where the thickness increased in the series deep morph, shallow morph, intermediate morph. The object from deep water was characterized by a clear lower value of *da*, *db* and *dc* and was clearly a thin-branching growth form when compared to the compact forms from lower depths. In all thickness measurements, the thickness of the intermediate morph was significantly characterized by a slightly larger mean thickness compared to the shallow water morph. In all thickness measurements the mean value of *dc* was significantly below the mean values of *da* and *db* (Table 1). All morphological measurements have also been compared using a nonparametric two-sample rank test (Table 2). The surface area and volume of each sample were measured, and the surface to volume ratio exhibited the opposite tendency of the branch thickness measurements, decreasing from the deep-water sample to the intermediate depth sample (Table 3).

Table 1 Results of measurements for diameter of *a*-, *b*- and *c*- spheres, branch spacing, branching angle, geotropy angle, and branching rate

| Measurement	Dataset	N	Median	Mean	SD	Skew	Kurtosis
Diameter of *a*, *b* and *c* spheres (*da*, *db*, and *dc*)							
Maximum thickness (mm)	Shallow	172	6.8	6.8	1.2	−0.08	−0.25
	Middle	175	7.3	7.4	1.4	0.02	−0.22
	Deep	65	5.5	5.7	1.2	0.49	−0.62
Minimum thickness (mm)	Shallow	345	5.4	5.5	1.6	−0.22	0.47
	Middle	351	5.9	5.9	1.9	−0.51	0.42
	Deep	131	4.4	4.7	1.3	0.82	0.49
End thickness (mm)	Shallow	173	4.2	4.1	1.3	−1.30	1.73
	Middle	176	4.5	4.2	1.7	−0.45	0.03
	Deep	66	3.2	3.2	0.8	−0.29	−0.39
Branch spacing (*br_spacing*)							
Degrees	Shallow	172	8.4	8.5	2.1	−0.16	−0.14
	Middle	175	9.9	9.9	3.1	0.10	−0.74
	Deep	65	11.6	11.8	4.2	0.40	−0.28
Branching angle (*b_angle*)							
Degrees	Shallow	172	88.8	90.9	21.9	0.21	0.11
	Middle	175	84.6	86.2	16.9	0.20	0.21
	Deep	65	89.4	91.0	13.6	0.29	−0.07
Geotrophy angle (*g_angle*)							
Degrees	Shallow	345	61.5	70.0	36.2	0.57	−0.30
	Middle	341	52.6	61.8	34.2	0.82	0.19
	Deep	131	70.4	71.5	33.8	0.53	0.34
Branching rate (*rb*)							
Degrees	Shallow	345	7.3	8.2	5.7	1.34	2.54
	Middle	341	9.9	11.0	7.9	1.059	1.30
	Deep	131	12.3	13.1	7.2	0.761	0.36

For histograms of measurements see Fig. 4

Discussion

This paper demonstrates that it is possible to analyze indeterminate growth forms in volumetric data sets stemming from an X-ray CT scanner by constructing a morphological skeleton. An important precondition for constructing a morphological skeleton is that the data set is preprocessed in such a way that all artifacts (for example cavities, holes in the skeleton, scanning artifacts, etc.) have been removed. For the morphologically variable coral *M. mirabilis*, these artifacts can be removed without compromising the major morphological characteristics of the colony. The visual interaction is a crucial step in the data processing and critically depends on the availability of morphological skeletons. Without these skeletons it is not possible to determine the various local morphological parameters (angles, thickness of branches, branching rates) in a useful way. Only a limited set of morphological characteristics has been discussed in this paper. By using the morphological skeleton as a "roadmap", there is a straightforward way to simplify the morphology (while preserving the topology) of the colony and a large variety of (local) morphological characteristics can be defined. The morphological skeleton can be used in a visual inspection of the data set, something that is required in many of the data processing steps, and the hierarchical structure of the skeleton can be used in various processing algorithms.

Currently the processing of a 3D image of a colony, including all visual inspection steps, takes approximately 1 h. The processing of the 3D data is the most time-consuming step and also depends on the complexity of the data set. The scanning process itself takes 2–3 min for the colony sizes investigated and for the type of scanner used in this study. In other 3D approaches, the data acquisition itself may take 2–3 h (Bythell et al 2001; Cocito et al 2003). In addition to the local morphological measurements, the computed morphological skeleton, the surface and the volume of the 3D image of the coral can be used to estimate the values of a series of global measurements: fractal dimensions characterizing the rugosity of the surface, the space-filling properties of the coral surface, space-filling properties of the morphological skeleton of the object, surface-volume ratios or the degree of compactness of the colony (see also Kaandorp et al. 2005). In general,
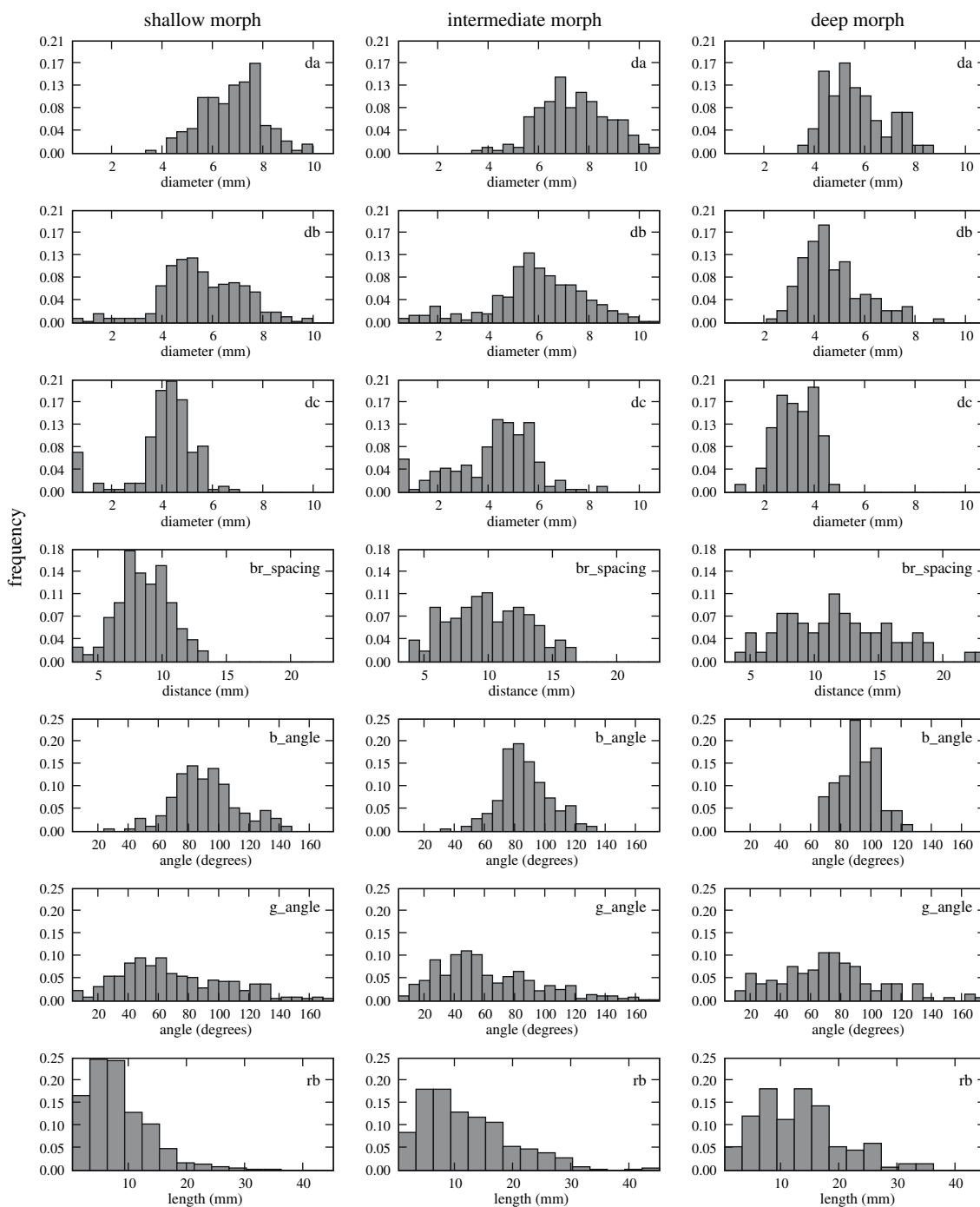
Fig. 4 Histograms for the measurements -diameter of *a*-, *b*- and *c*- spheres (*da*, *db* and *dc*), the branch spacing (*br_spacing*), branching angle (*b_angle*), geotropy angle (*g_angle*) and branching rate *(rb)*. The histograms show the values of the measurements on the *x*-axis, and the frequency distribution of these values on the *y*-axis. From *top* to *bottom*, each set of histograms shows the distribution the measurements of *da, db, dc, br_spacing, b_angle, g_angle,* and *rb* for respectively, the colonies from shallow, intermediate depth and deep water. All thickness and distance measurements *da, db, dc, br_spacing* and *rb* are in mm, all angles *b_angle* and *g_angle* are in degrees

the local morphological characteristics, as for example *br_spacing*, can be more easily linked to biological properties of the objects, while global characteristics lump together many different morphological properties into one number. Potentially the surface–volume estimations can be used to calibrate field methods available for 3D morphometrics of complex-shaped marine sessile organisms (Bythell et al 2001; Cocito et al 2003).

This analysis demonstrates that it is possible to quantify a range of morphological characteristics in the samples, to

Table 2 Results of a two-sample rank test for the distributions of the measurements of two objects

Measurement	Shallow and middle	Shallow and deep	Middle and deep
Maximum thickness	<	>	>
Minimum thickness	<	>	>
End thickness	0	>	>
Branch spacing	<	<	<
Branching angle	>	0	<
Geotropy angle	>	0	<
Branching rate	<	<	0

'<' distribution of object 1 is located to the left of object 2; '0' distribution of both objects is the same; and '>' distribution of object 1 is located to the right of object 2

Table 3 Surface (cm^2), volume (cm^3), and surface/volume ratios of the samples

Object	Volume segmentation (cm^3)	Volume iso-surface (cm^3)	Area iso-surface (cm^2)	Surface/ volume ratio
Shallow	104.1	97.8	59.8	0.61
Middle	185.1	173.0	100.2	0.57
Deep	44.2	40.9	31.3	0.77

construct a morphological "fingerprint" of a certain morph, and to compare it to other growth forms. In all thickness measurements the mean value of *dc* was significantly below the mean values of *da* and *db*, although it would be expected that *dc* is located between the mean values of *da* and *db*. In a branching coral without tapering ends the thickness of the branches will be the largest at the point of branching and the smallest immediately after branching. Here it should be noted that the value of *dc* strongly depends on the skeletonization algorithm (Kruszyński et al. 2005) and the determination of the endpoints. Another explanation here is that the tips of the colony are initially somewhat tapered in the growth process. In the deep water sample shown in Fig. 3c the tips of the colony exhibit some tapering. The degree of regularity of a branching pattern can be determined by considering the variation of the branch spacing (*br_spacing*) and the branching rate (*rb*), with low variation indicating a regular pattern. Furthermore, the values of *br_spacing* indicate if there is any fusing of branches in the sample. For example for the deep water object there are no values close to zero, which demonstrates that there is no anastomosis, which is an important biological property. It is possible to detect and quantify branch fusing, but to our knowledge there is no algorithm available for detecting the exact location of anastomosis. This analysis method requires the detected fusing to be manually removed. For organisms with a high degree of

anastomosis this might increase the time taken to complete sample analysis. The variation of the geotropy angles (*g_angle*) quantifies if branches tend to form in almost all directions. Quite remarkable is that the mean value of the branching angle (*b_angle*) is nearly similar in the three objects, which corresponds to an earlier observation (Kaandorp 1999) that *b_angle* might be a morphological invariant in branching corals. The standard deviation of *b_angle* decreased with increasing sample depth, which demonstrates that *b_angle* is probably in practice not very useful as a morphological invariant characterizing for example a certain species and that there may be a physical/biomechanical explanation for this phenomenon.

The major result is that an interactive system for the quantitative analysis of complex-shaped branching organisms has been developed. This technique has been tested in a branching scleractinian coral but the same method can be applied to other marine sessile organisms and biological structures. The method can be used to measure the morphology of 3D objects with a simple geometry, as well as samples with an arbitrarily complex branching morphology, with a very high precision. Complex-shaped branching morphologies cannot be measured using other currently available 3D techniques (Bythell et al 2001; Cocito et al 2003).

References

Abraham ER (2001) The fractal branching of an arborescent sponge. Mar Biol 138:503–510

Bookstein FL (1991) Morphometric tools for landmark data: geometry and biology. Cambridge University Press, New York

Bruno JF, Edmunds PJ (1998) Metabolic consequences of phenotypic plasticity in the coral *Madracis mirabilis* (Duchassaing and Michelotti): the effect of morphology and water flow on aggregate respiration. J Exp Mar Biol Ecol 229:187–195

Budd AF, Guzman HM (1994) *Siderastrea glynni*, a new species of scleractinian coral (Cnidaria: Anthozoa) from the eastern pacific. Proc Biol Soc Wash 107:591–599

Budd AF, Johnson KG, Potts DC (1994) Recognizing morphospecies in colonial reef corals: I. Landmark-based methods. Paleobiology 20:484–505

Bythell JC, Pan P, Lee J (2001) Three-dimensional morphometric measurements of reef corals using underwater photogrammetry techniques. Coral Reefs 20:193–199

Cocito S, Sgorbini S, Peirano A, Valle M (2003) 3–D reconstruction of biological objects using underwater video technique and image processing. J Exp Mar Biol Ecol 279:57–70

Graus RR, Macintyre IG (1982) Variation in growth forms of the reef coral *Montastrea annularis* (Ellis and Solander): a quantitative evaluation of growth response to light distribution using computer simulation. Smithson Contrib Mar Sci 12:441–464

Harper JL, Rosen BR, White J (1986) The growth and form of modular organisms. The Royal Society London, London

Hoegh-Guldberg O (1988) A method for determining the surface area of corals. Coral Reefs 7:113–116

Horton RE (1945) Erosional development of streams and their drainage basins: hydrophysical approach to quantitative morphology. Geol Soc Am Bull 56:275–370

Ibanez L, Schroeder W (2003) The ITK Software Guide. Kitware Inc., Clifton Park

Jonker PP, Vossepoel AM (1995) Mathematical morphology in 3D images: comparing 2D & 3D skeletonization algorithms. Proceedings BENEFIT Summer School on Morphological Image and Signal Processing, Zakopane. Silesian Technical University, ACECS, Gliwice, pp 83–108

Kaandorp JA (1999) Morphological analysis of growth forms of branching marine sessile organisms along environmental gradients. Mar Biol 134:295–306

Kaandorp JA (2007) Modelling and analysis of growth and form of sponges and scleractinian corals. http://www.science.uva.nl/research/scs/GF2004/

Kaandorp JA, de Kluijver MJ (1992) Verification of fractal growth models of the sponge *Haliclona oculata* (Porifera; class Demospongiae) with transplantation experiments. Mar Biol 113:133–143

Kaandorp JA, Kübler JE (2001) The algorithmic beauty of seaweeds, sponges and corals. Springer, Heidelberg

Kaandorp JA, Koopman EA, Sloot PMA, Bak RPM, Vermeij MJA, Lampmann LEH (2003) Simulation and analysis of flow patterns around the scleractinian coral *Madracis mirabilis* (Duchassaing and Michelotti). Philos Trans R Soc Lond B 358:1551–1557

Kaandorp JA, Sloot PMA, Merks RMH, Bak RPM, Vermeij MJA, Maier C (2005) Morphogenesis of the branching reef coral *Madracis mirabilis*. Proc R Soc Lond B 272:127–133

Kim E, Lasker HR, Coffroth MA, Kim K (2004) Morphological and genetic variation accross reef habitats in broadcast-spawning octocoral. Hydrobiologia 530/531:423–432

Kruszyński KJ, van Liere R, Kaandorp JA (2005) Quantifying differences in skeletonization algorithms: a case study. Proceedings 5th IASTED International Conference on Visualization, Imaging, and Image Processing, Benidorm, Spain. IASTED, Calgary, Canada, pp 666–673

Kruszyński KJ, van Liere R, Kaandorp JA (2006) An interactive visualization system for quantifying coral structures. Proceedings Eurographics/IEEE VGTC Symposium on Visualization (EuroVis 2006), Lisbon, Portugal, pp 283–290

Lesser MP, Weis VM, Patterson MR, Jokiel PL (1994) Effects of morphology and water motion on carbon delivery and productivity in the reef coral, *Pocillopora damicornis* (Linnaeus): diffusion barriers, inorganic carbon limitation, and biochemical plasticity. J Exp Mar Biol Ecol 178:153–179

Marsh JA (1970) Primary productivity of reef-building calcareous algae. Ecology 51:255–263

Merks RMH, Hoekstra AG, Kaandorp JA, Sloot PMA (2003) Models of coral growth: spontaneous branching, compactification and the Laplacian growth assumption. J Theor Biol 224:153–166

Meyers JL, Schultz ET (1985) Tissue condition and growth rate of corals associated with schooling fish. Limnol Oceanogr 30:157–166

Muko S, Kawasaki K, Sakai K, Takasu F, Shigesada N (2000) Morphological plasticity in the coral *Porites sillimaniani* and its adaptive significance. Bull Mar Sci 66:225–239

Reinders S, Jacobson MED, Post FH (2000) Skeleton graph generation for feature shape description. Proceedings Eurographics/IEEE VGTC Symposium on Visualization (VisSym 2000), Amsterdam, The Netherlands, pp 73–82

Sanchez JA, Lasker HR (2003) Patterns of morphological integration in marine modular organisms: supra-module organization in branching octocoral colonies. Proc R Soc Lond B 270:2039–2044

Schroeder W, Martin K, Lorensen B (1997) The visualization toolkit: an object-oriented approach to 3D graphics, 2nd edn. Prentice Hall, New Jersey

Sebens KP, Witting J, Helmuth B (1997) Effects of water flow and branch spacing on particle capture by the reef coral *Madracis mirabilis* (Duchassaing and Michelotti). J Exp Mar Biol Ecol 211:1–28

Shaish L, Abelson A, Rinkevich B (2006) Branch to colony trajectory in a modular organism: pattern formation in the Indopacific coral *Stylophora pistillata*. Dev Dynam 235:2111–2121

Stearn CW, Riding R (1973) Forms of the hydrozoan *Millepora* on a recent coral reef. Lethaia 6:187–200

Stimson J, Kinzie RA (1991) The temporal pattern and rate of release of zooxanthellae from the reef coral *Pocillopora damicornis* (Linnaeus) under nitrogen-enrichment and control conditions. J Exp Mar Biol Ecol 153:63–74

Todd PA, Sanderso PG, Chou LM (2001) Morphological variation in the polyps of the scleractinian coral *Favia speciosa* (Dana) around Singapore. Hydrobiologia 444:227–235

Vago R, Shai Y, Ben-Zion M, Dubinsky Z, Achituv Y (1994) Computerized tomography and image analysis: a tool for examining the skeletal characteristics of reef-building organisms. Limnol Oceanogr 39:448–452

de Weerdt WH (1981) Transplantation experiments with Caribbean *Millepora* species (Hydrozoa, Coelenterata), including some ecological observations on growth forms. Bijdr Dierkd 51:1–19

Xie W, Thompson R, Perucchio R (2003) A topology-preserving parallel 3D thinning algorithm for extracting the curve skeleton. Pattern Recogn 36:1529–1544